Journal of Materials and Environmental Sciences
ISSN : 2028-2508
CODEN : JMESCN

J. Mater. Environ. Sci., 2018, Volume 9, Issue 7, Page 2071-2086

http://www.jmaterenvironsci.com

Evaluation of the NO-NO_2-O_3 photostationary state in roadside environments of Agadir city, (southwestern of Morocco)

M. El Abassi[1], H. El Haddaj[1], J. Damich[3], B. Hanoune[2], L. El Maimouni[1*]

[1]*Laboratoryof Chemistry Materials and Physical Chemistry of the Atmosphere and Climate, Faculty of Science, Ibn Zohr University, BP 8106, 80000 Agadir, Morocco*

[2]*Univ. Lille, CNRS, UMR 8522 - PC2A - Physicochimie des Processus de Combustion et de l'Atmosphère, F-59000 Lille, France*

[3]*Service Transport & Mobibilité urbains, Commune Urbaine d'Agadir, Maroc*

Received 10 Jan 2018,
Revised 20 May 2018,
Accepted 26 May 2018

Keywords
- ✓ NOx and O_3
- ✓ polution,
- ✓ tailpipe emissions,
- ✓ Modeling,

elmaimounil@yahoo.fr ;
Phone: +212662078337;

Abstract

In this study, we measured the NOx and O_3 concentrations in different roadsides places, and one background site, in the city of Agadir, Southern Morocco, between January 2014 and June 2015. The observed concentrations were used to investigate whether the assumption that the photostationary state was reached, implicitly used in the air quality predictive models, was holding true. To our knowledge, this is the first time that this assumption is tested in roadside environments. Only in the background site, far from the direct traffic emissions, could the atmosphere considered in photostationary equilibrium. For the traffic sites, the excess NO from the tailpipe emissions does not have time to react or to be perfectly mixed with the background pollutants, leading to a significant deviation from the photostationary equilibrium. We suggest that the measured concentration ratio NO_2/NO may be used as a criterion to evaluate the photostationary state of the urban atmosphere, which could be taken into account both for field measurements and for modeling purposes.

1. Introduction

Modeling is one of the main tools for the predictive investigation of air quality, in particular in urban areas. Understanding the roadside environments requires overcoming the many difficulties engendered by the multifactorial character of pollution, which involves a large number of factors such as the local emissions from vehicle exhaust, the traffic conditions, the composition of the vehicle fleet, the local weather conditions and the design of the roads. As measuring continuously the air quality parameters in every point of interest is not possible, numerical modeling can be used to reproduce the monitored or expected levels of pollutants at different points. The convergence between the calculated and observed concentration levels is the first step before the model can be used to simulate the evolution of the air quality according to possible future scenarios.

The time scales associated to pollutant transfer over and within urban atmospheres vary from a few minutes to several hours [1], and a large number of chemical reactions must be taken into account to predict correctly the pollutant levels in the studied areas [2]. However, if we consider only the timescales associated to the local dispersion of pollutants, i.e. at close proximity of the emission sources, the characteristic times are considerably reduced and most of the chemical reactions can be neglected. There are however reactions which are sufficiently rapid to modify significantly the concentration of some pollutants in urban areas. This is the case in particular for the nitrogen oxides NOx which result principally from combustion processes. It is commonly considered that the repartition of NOx at the emission is about 10-15% of NO_2 and 85-90% of NO [3]. However, since the chemical reactions in air convert NO into NO_2, it is necessary that an urban dispersion model includes a module to take into account the conversion of NO into NO_2.

Several approaches have been adopted to study urban atmospheres at the local scale. Liu and Leung [4] applied a chemistry box model to simulate VOC and NOx levels within a street canyon, focusing on the case of calm wind conditions. Another approach was adopted by Mensik and Cosemans [5], who coupled the OSPM street canyon model to a Gaussian dispersion model for the prediction of background levels. In recent years, more sophisticated models have been adopted. This is the case of Baker et al. [6] who used a large eddy

simulation code to simulate transfer of reactive pollutant at street scales. Even if large parts of the current models are based on highly simplified assumptions, they provide sufficiently accurate estimates for operational purposes. A review on the performances of different models can be found in [7]. Another comparison of the performances of the different dispersion and chemical models was conducted by Hirtl and Baumann-Stanzer [8], who analyzed the outputs of the Gaussian model ADMS-Roads coupled to the Lagrangian model LASAT.

One of the main assumptions is the establishment of a photochemical equilibrium, or photostationary state (PSS), that will govern the NOx (NO and NO_2) and O_3 concentrations, through the Leighton cycle [9,10] (reactions R1 to R3):

R1: $NO_2 + h\nu$ (λ<420 nm) → $NO + O(^3P)$, with a photolysis rate constant J_{NO2} (s^{-1})

R2: $O(^3P) + O_2 \rightarrow O_3$; $k_2 = 2.8\times10^{-12}$ cm^3 $molecule^{-1}$ s^{-1} [11]

R3: $NO + O_3 \rightarrow NO_2 + O_2$; $k_3 = 1.65\times10^{-14}$ cm^3 $molecule^{-1}$ s^{-1} [12]

This cycle takes into account the photolysis of NO_2 by solar UV (λ < 420 nm), which is one of the key photochemical processes of the atmosphere [13] and is therefore an important parameter in all the photochemical models (Gaussian model ADMS-Roads, Lagrangian model LASAT, AERMOD, SIRANE...). The photodecomposition of NO_2 leads to NO molecules and ground-state $O(^3P)$ oxygen atoms that can combine with molecular oxygen to produce ozone, which in turn can react with NO forming NO_2.
The photolysis rate constant J_{NO2}, of the order of a few 10^{-3} s^{-1}, depends upon the intensity of solar light. It can be expressed as [14]:

$$J_{NO2}\ (s^{-1}) = \frac{1}{60}\left(0.5699 - \left[9.056\times10^{-3}\left(90 - \phi_{solar}\right)\right]^{2.546}\right)\left(1 - 0.75\left(\frac{Cld}{8}\right)^{3.4}\right) \qquad \text{(Eq.1)}$$

where ϕ_{solar} is the solar elevation (°) and *Cld* the cloud coverage (%).
The rate constant k_3 for reaction R3 depends only upon the temperature *T* (K) of ambient air and can be expressed as [15]:

$$k_3\,(cm^3\ molecule^{-1}s^{-1}) = 1.4\times10^{-12}\exp\left[\frac{-1310}{\tau}\right] \qquad \text{(Eq.2)}$$

A convenient way to verify whether the photostationary state (PSS) is reached resides with the calculation of the dimensionless photostationary parameter ρ:

$$\rho = \frac{J_{(NO_2)}[NO_2]}{k_s[O_s][NO]} \qquad \text{(Eq.3)}$$

When the PSS is reached, then ρ takes the value of 1. This assumption of a photochemical equilibrium however holds true only when possible competing reactions such as the ones between nitrogen oxides and VOCs or reactive radical species (RO_2, HO_2) can be neglected. This normally prevents the use in the model of measurement data taken from the curbside, which would be strongly influenced by the traffic emissions. Still, these curbside data sometimes constitute the only available data and have to be used as input.

On another hand, it is rare when the PSS equilibrium is reached [1,16,17], and in many studies, in urban or remote zones [18-20], ρ values have been found that significantly lower or higher than 1, indicative of nearby sources, additional chemical reactions, and/or insufficient mixing of the air masses.

In the present paper, we measured NOx and O_3 concentrations at five roadside sites and one background site in Agadir city (Morocco) and investigated the validity of the photochemical equilibrium assumption on which the numerical models are based, through the comparison of the $[NO][O_3]/[NO_2]$ ratio measured and of the J_{NO2}/k_3 ratio calculated taking into account the dependence on the environmental parameters (ambient air temperature, solar elevation and cloud coverage factor). This is to our knowledge the first time that the influence of the proximity of the traffic on the deviation to the PSS assumption is investigated.

2. Experimental section

2.1 General description of the study zone

The urban community of Agadir (Figure 1), counting over 420,000 inhabitants [21], is located at 30°56'N, 9°13'W. It is the largest city of southern Morocco. The climate is semi-arid to arid, influenced by several factors: the Atlas mountain range, the Atlantic Ocean coast. The average annual rainfall is about 260 mm. The annual average maximum and minimum temperatures are 27 °C (August) and 11 °C (January) respectively, with a relative humidity ranging between 32% and 85%. The wind is mostly in the west-

northwest direction, with a wind speed ranging from 0.1 to 3.3 $m.s^{-1}$. As already stressed in our previous papers [22-23], these specific meteorological conditions can create a temperature inversion leading to an accumulation of pollutants in the lower layer of the atmosphere.

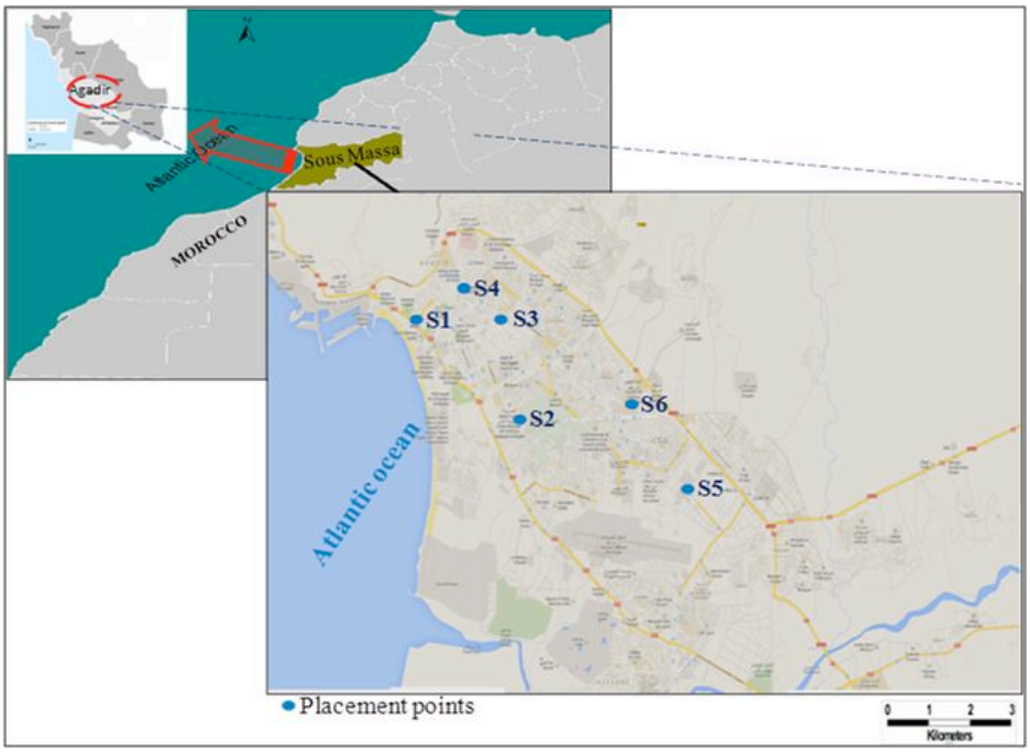

Figure 1: *Map of Agadir city indicating the placement of the measurements points (S1-S6)*

2.2. Position and *description of the sampling sites*

We selected six sites in the Agadir area. Sites S1 to S5 are roadsides sites. Site S6 is located at Agadir Faculty of Science, far from any direct traffic influence, and can be considered as a background site. The locations of the measurements points are shown on Figure.1. Table 1 describes their characteristics and their immediate environments.

Table 1: Characteristics of the selected measurements points

Site	Coordinates	Placement and description
S1	30°25'16.9"N 9°36'20.2"W	Near the Wilaya of the Agadir, at the intersection of El Kettani and Mohamed V avenues. Intense traffic in the daytime. Strongly influenced also by air masses coming from the seaside. Presents therefore a higher relative humidity than the other sites.
S2	30°24'11.6"N 9°34'50.3"W	Near of Appeal Court of Agadir. High traffic flow crossing the East-West Road
S3	30°25'17.9"N 9°34'58.1"W	Near the old industrial zone of Agadir at the intersection of Mohamed Saadi Cheikh and Kadi Ayad boulevards.
S4	30°25'39.6"N 9°35'31.7"W	At the intersection of the FAR and Mohammed Cheikh Saadi avenues. Surrounded by low rise buildings. Intense vehicle traffic.
S5	30°23'26.4"N 9°31'46.4"W	On the daily transit road (Avenue Al Farabi) connecting Agadir to Inezgane city. Intense traffic from and to Agadir. To the difference of Sites S1 to S4, this road has buildings only on one side (no canyon effect). Vertical and horizontal dilution is very important.
S6	30°24'21.5"N 9°32'40.0"W	Located at the center of the Faculty of Science of Agadir. Far from any direct influence of industrial and traffic emissions.

Table 2: Daily average temperature, relative humidity and wind speed recorded in Agadir

Site	Date	T (°C)	RH (%)	wind speed (m/s)
S1	06/06/2014	21	88.3	3.3
	11/06/2014	24	62.7	3.2
	18/06/2014	23	67.6	3.4
S2	06/01/2014	18	72.6	3.7
	03/02/2014	16	79.1	2.8
	10/06/2014	24	62.7	2.9
	19/06/2014	22	72.2	2.4
S3	03/01/2014	16	74.4	3.4
	25/01/2014	17	66.1	3.2
	08/02/2014	16	74.4	3.5
S4	04/01/2014	16	76.1	2.3
	26/01/2014	17	70.1	2.9
	06/02/2014	16	82.7	4.1
S5	17/01/2015	15	71.8	1.6
	27/01/2015	13	84.8	2.7
	17/02/2015	17	65.8	3.6
S6	23/02/2015	17	76.0	2.4
	24/02/2015	19	83.6	2.5
	25/02/2015	18	78.5	2.3

2.3. Measurements of NO, NO^2 and O_3

In each site, ozone (O_3) and NOx (NO and NO_2) were measured simultaneously using online gas analyzers (Environnement SA model 41M for ozone, based on UV absorption at 253.7 nm, detection limit 0.4 ppb ; Environnement SA model 31M for NOx, based on chemiluminescence, detection limit 0.35 ppb). Measurements were taken every 15 minutes. The sampling point was placed at a height of 4 m above the ground, 10 to 120 m away from the roadside.

3. Results

For each measurement point, the NOx and O_3 concentrations measured and the meteorological parameters (temperature and cloud coverage at Agadir Al Massira airport, and solar elevation calculated using a tool available on http://www.sunearthtools.com/) are listed in Tables 3 to 8. Also given in these tables are the calculated rate constant k_3, NO_2 photolysis frequency J_{NO2}, and the derived ρ values, which will be discussed below.

The ratio J_{NO2}/k_3, calculated from the temperature, solar elevation and cloud coverage, using the two equations (Eq 1) and (Eq 2), is independent of the site under investigation, because of the proximity of the measurement points. This ratio starts from 0 at sunrise, reaches a maximum of ~20 ppb between 12:00-13:00, and reverts to 0 at sunset, because it is driven mainly by the solar elevation, with only a minor correction induced by the cloud coverage.

For the background site S6, the concentrations of nitrogen oxides remain low throughout the days, with NO between 13 and 21 ppb and NO_2 between 20 and 30 ppb. At the same time, ozone concentrations range between 10 to 37 ppb. This corresponds to the background pollution levels over the Agadir City area. For the sites close to the traffic, the O_3 concentrations are in the same order as in the background site, between 20 and 30 ppb in winter and up to 40 ppb in summer, but nitrogen oxide concentrations are much higher, confirming the influence of the traffic emissions. Individual variations between the sites, or for a given site between the days of measurements, are linked to different traffic patterns, intensity of the traffic, and temporary congestions. No counting of the vehicles was performed simultaneously with the pollutant measurements to precise these points. The distance of the measurement point to the main roads at the sampling site also directly impacts the measured concentration, for instance for site 1 on June 11 when the sampling point was further away (about 100 m) because of electrical power availability than on the other days (about 20 m). No specific difference between the measurements carried out in winter (January and February) and in summer (June) can be put in evidence.

Table 3: Measured concentrations, meteorological data, and derived rate constants and equilibrium parameter for roadside environment (site S1).

Site	Date	Time	O_3	NO	NO_2	T	Cld	Elevation	$J_{NO2}\times10^3$	$k_3\times10^{14}$	$10^{-11}\times([O_3]\,[NO]/[NO_2])$	$10^{-11}\times J_{NO2}/k_3$	ρ
			(ppb)	(ppb)	(ppb)	(°C)	(%)	Θ (°)	(s^{-1})	($cm^3 molecule^{-1} s^{-1}$)	(molecule cm^{-3})	(molecule cm^{-3})	
S1	06/06/2014	08:00	22	119	50	18	25	28.47	5.74	1.56	12.74	3.69	0.289
		09:00	25	122	53	18	22	41.28	7.42	1.57	14.02	4.74	0.338
		10:00	20	194	80	19	18	54.20	8.55	1.58	12.14	5.43	0.447
		11:00	27	85	72	20	20	67.00	9.19	1.60	7.78	5.73	0.736
		12:00	25	96	80	21	19	78.65	9.45	1.63	7.28	5.80	0.797
		13:00	24	90	70	22	16	80.72	9.47	1.65	7.49	5.75	0.768
		14:00	29	86	74	23	12	69.96	9.28	1.68	8.30	5.53	0.666
		15:00	30	87	75	24	7	57.27	8.74	1.70	8.57	5.13	0.599
		16:00	32	94	58	23	10	44.35	7.74	1.67	12.60	4.64	0.368
		17:00	26	228	77	23	25	31.51	6.19	1.68	18.92	3.69	0.195
		18:00	25	250	80	22	27	18.89	4.06	1.65	19.37	2.46	0.127
S1	11/06/2014	08:00	22	45	42	18	22	28.44	5.73	1.56	5.67	3.68	0.650
		09:00	23	41	41	19	21	41.23	7.42	1.59	5.71	4.67	0.819
		10:00	26	48	44	21	14	54.15	8.55	1.62	7.23	5.27	0.729
		11:00	35	37	39	22	12	66.97	9.19	1.65	8.20	5.56	0.677
		12:00	36	52	47	24	11	78.79	9.45	1.70	9.85	5.54	0.563
		13:00	24	88	72	25	10	81.20	9.47	1.73	7.25	5.47	0.754
		14:00	24	91	69	27	9	70.35	9.29	1.78	7.66	5.22	0.681
		15:00	31	67	48	27	11	57.63	8.77	1.78	10.75	4.92	0.458
		16:00	32	89	62	27	11	44.71	7.77	1.77	11.15	4.40	0.394
		17:00	30	106	70	26	12	31.87	6.24	1.76	11.00	3.56	0.323
		18:00	23	142	74	26	18	19.28	4.14	1.76	10.67	2.36	0.221
S1	18/06/2014	08:00	25	134	52	20	16	28.25	5.70	1.60	15.79	3.55	0.225
		09:00	19	110	45	21	17	41.02	7.39	1.64	11.16	4.52	0.405
		10:00	19	159	58	22	14	53.94	8.53	1.65	12.62	5.16	0.409
		11:00	18	122	69	23	12	66.78	9.18	1.68	7.64	5.47	0.716
		12:00	21	216	81	24	10	78.74	9.45	1.69	14.01	5.58	0.398
		13:00	26	95	65	26	10	81.64	9.47	1.76	9.40	5.40	0.574
		14:00	31	92	69	25	8	70.79	9.30	1.73	10.24	5.38	0.525
		15:00	32	93	70	25	11	58.06	8.79	1.73	10.53	5.09	0.483
		16:00	25	141	97	24	14	45.14	7.82	1.70	8.97	4.59	0.511
		17:00	26	252	67	23	12	32.30	6.31	1.68	24.34	3.76	0.154
		18:00	25	250	80	22	10	19.71	4.22	1.66	19.40	2.54	0.131

Table 4: Measured concentrations, meteorological data, and derived rate constants and equilibrium parameter for roadside environment (site S2).

Site	Date	Time	O_3	NO	NO_2	T	Cld	Elevation	$J_{NO2}\times10^3$	$k_3\times10^{14}$	$10^{-11}\times([O_3]\,[NO]/[NO_2])$	$10^{-11}\times J_{NO2}/k_3$	ρ
			(ppb)	(ppb)	(ppb)	(°C)	(%)	Θ (°)	(s^{-1})	(cm^3 $molecule^{-1}$ s^{-1})	(molecule cm^{-3})	(molecule cm^{-3})	
		08:00	24	31	21	6	91	3.76	0.61	1.28	8.59	0.48	0.056
		09:00	25	42	25	10	94	14.58	3.18	1.36	10.02	2.33	0.233
		10:00	25	21	17	16	89	24.06	5.01	1.51	7.33	3.32	0.453
		11:00	26	60	33	20	89	31.51	6.19	1.60	11.71	3.86	0.329
S2	06/01/2014	12:00	27	46	22	23	72	36.07	6.81	1.68	13.80	4.04	0.293
		13:00	27	51	21	25	55	37.00	6.93	1.73	16.07	4.00	0.249
		14:00	28	70	41	21	20	34.09	6.55	1.63	11.79	4.02	0.341
		15:00	23	67	46	21	54	27.90	5.65	1.62	8.44	3.48	0.412
		16:00	22	64	42	20	41	19.29	4.14	1.60	8.28	2.58	0.311
		17:00	15	71	51	20	28	9.04	1.94	1.60	5.22	1.21	0.231
		08:00	25	33	28	12	80	5.60	1.09	1.42	7.03	0.77	0.110
		09:00	26	45	34	13	80	17.10	3.71	1.44	8.37	2.57	0.307
		10:00	31	32	29	15	52	27.45	5.58	1.49	8.38	3.76	0.448
		11:00	33	56	40	16	52	35.91	6.79	1.50	11.26	4.50	0.400
		12:00	32	46	37	17	24	41.49	7.45	1.54	9.90	4.84	0.488
S2	03/02/2014	13:00	34	48	32	19	22	43.11	7.62	1.58	12.71	4.82	0.379
		14:00	41	35	31	18	20	40.40	7.33	1.56	11.47	4.71	0.410
		15:00	37	36	32	18	34	33.98	6.54	1.56	10.31	4.19	0.406
		16:00	23	64	48	18	38	24.94	5.16	1.56	7.65	3.32	0.433
		17:00	17	109	56	17	41	14.25	3.11	1.53	8.24	2.03	0.246
		18:00	15	177	107	16	44	2.52	0.28	1.50	6.18	0.19	0.031
		08:00	23	35	35	18	61	20.19	4.31	1.56	5.62	2.77	0.492
		09:00	26	48	44	20	55	32.97	6.40	1.60	7.18	3.99	0.555
		10:00	36	44	41	21	57	45.23	7.82	1.63	9.38	4.79	0.511
		11:00	36	52	47	23	12	56.22	8.68	1.67	9.85	5.21	0.528
		12:00	39	46	52	24	10	64.09	9.08	1.70	8.48	5.33	0.628
S2	10/06/2014	13:00	40	46	42	25	10	65.54	9.14	1.72	10.78	5.32	0.493
		14:00	38	57	49	26	20	59.63	8.88	1.76	10.87	5.06	0.465
		15:00	33	59	50	27	35	49.50	8.20	1.78	9.80	4.61	0.470
		16:00	29	49	48	27	40	37.59	7.00	1.78	7.21	3.94	0.547
		17:00	36	46	43	27	21	24.95	5.17	1.78	9.46	2.90	0.307
		18:00	22	69	54	25	21	12.05	2.63	1.73	6.87	1.52	0.221
		08:00	27	53	31	18	19	28.23	5.70	1.56	11.43	3.66	0.320
		09:00	31	68	45	20	17	41.00	7.39	1.60	1.1.62	4.61	0.397
		10:00	36	60	45	21	15	53.92	8.53	1.63	11.95	5.24	0.439
		11:00	30	84	45	22	12	66.77	9.18	1.66	13.57	5.55	0.409
		12:00	32	84	59	23	11	78.74	9.45	1.68	11.30	5.63	0.498
S2	19/06/2014	13:00	33	76	48	23	10	81.69	9.48	1.68	12.67	5.63	0.444
		14:00	42	63	47	24	9	70.82	9.30	1.70	13.78	5.46	0.396
		15:00	42	69	53	25	12	58.09	8.79	1.73	13.67	5.08	0.372
		16:00	25	84	53	24	13	45.17	7.82	1.70	9.67	4.59	0.474
		17:00	21	134	61	24	12	32.33	6.31	1.70	11.21	3.70	0.330
		18:00	19	202	112	23	11	19.74	4.23	1.68	8.29	2.52	0.303

Table 5: Measured concentrations, meteorological data, and derived rate constants and equilibrium parameter for roadside environment (site S3).

Site	Date	Time	O_3	NO	NO_2	T	Cld	Elevation	$J_{NO2}\times10^3$	$k_3\times10^{14}$	$10^{-11}\times([O_3]\,[NO]/[NO_2])$	$10^{-11}\times J_{NO2}/k_3$	ρ
			(ppb)	(ppb)	(ppb)	(°C)	(%)	Θ (°)	(s^{-1})	(cm^3 $molecule^{-1}$ s^{-1})	(molecule cm^{-3})	(molecule cm^{-3})	
		08:00	21	86	45	5	71	3.81	0.63	1.26	9.86	0.50	0.051
		09:00	22	84	49	8	59	14.57	3.18	1.32	9.16	2.4	0.264
		10:00	22	89	40	13	39	23.97	5.00	1.44	12.32	3.47	0.282
		11:00	29	90	58	17	12	31.33	6.17	1.53	11.18	4.02	0.360
S3	03/01/2014	12:00	30	111	66	20	10	35.79	6.77	1.61	12.46	4.20	0.337
		13:00	29	98	61	21	31	36.62	6.88	1.63	11.51	4.22	0.367
		14:00	28	78	52	21	20	33.66	6.49	1.62	10.19	3.99	0.391
		15:00	35	65	61	20	56	27.44	5.58	1.61	9.38	3.46	0.369
		16:00	29	86	64	20	34	18.83	4.05	1.60	9.49	2.52	0.266
		17:00	25	78	60	19	21	8.58	1.83	1.58	8.11	1.16	0.142
		08:00	19	79	46	8	80	4.51	0.81	1.32	8.09	0.61	0.076
		09:00	21	76	50	12	60	15.78	3.44	1.41	7.92	2.43	0.307
		10:00	17	82	41	16	40	25.82	5.31	1.50	8.22	3.52	0.428
		11:00	23	82	59	19	30	33.94	6.53	1.58	8.12	4.13	0.509
S3	25/01/2014	12:00	24	108	74	20	30	39.19	7.19	1.60	8.75	4.49	0.513
		13:00	23	91	62	21	35	40.63	7.35	1.63	8.41	4.51	0.536
		14:00	28	77	52	21	20	37.95	7.04	1.63	9.99	4.32	0.432
		15:00	33	62	56	20	38	31.71	6.22	1.61	9.18	3.85	0.420
		16:00	27	83	54	19	34	22.92	4.81	1.58	10.10	3.05	0.301
		07:00	23	81	60	19	21	12.44	2.72	1.58	7.61	1.72	0.226
		08:00	21	45	35	8	45	6.37	1.28	1.33	6.39	0.97	0.152
		09:00	23	78	54	11	51	18.01	3.89	1.40	8.16	2.79	0.342
		10:00	20	84	44	14	24	28.52	5.75	1.47	9.41	3.93	0.418
		11:00	27	85	62	16	34	37.17	6.95	1.51	9.04	4.61	0.510
		12:00	28	106	70	18	34	42.93	7.60	1.59	1.03	4.87	0.473
S3	08/02/2014	13:00	27	93	65	19	41	44.63	7.77	1.58	9.38	4.91	0.524
		14:00	29	86	64	18	20	41.86	7.49	1.57	9.60	4.81	0.501
		15:00	30	87	65	18	38	35.29	6.71	1.55	9.89	4.33	0.438
		16:00	30	81	63	18	33	26.09	5.36	1.57	9.57	3.44	0.360
		07:00	25	104	73	18	38	15.26	3.33	1.57	8.77	2.14	0.244
		18:00	22	118	76	17	44	3.42	5.27	1.52	8.32	0.35	0.042

Table 6: Measured concentrations, meteorological data, and derived rate constants and equilibrium parameter for roadside environment (site S4).

Site	Date	Time	O_3	NO	NO_2	T	Cld	Elevation	$J_{NO2}\times10^3$	$k_3\times10^{14}$	$10^{-11}\times([O_3]\,[NO]/[NO_2])$	$10^{-11}\times J_{NO2}/k_3$	ρ
			(ppb)	(ppb)	(ppb)	(°C)	(%)	Θ (°)	(s^{-1})	(cm^3 $molecule^{-1}$ s^{-1})	(molecule cm^{-3})	(molecule cm^{-3})	
S4	04/01/2014	08:00	21	51	33	4	59	3.77	0.62	1.24	7.89	0.50	0.063
		09:00	25	36	28	7	59	14.56	3.18	1.31	7.95	2.43	0.305
		10:00	29	65	39	13	56	23.98	5.00	1.44	12.11	3.48	0.287
		11:00	26	75	49	16	12	31.37	6.17	1.51	9.74	4.09	0.420
		12:00	27	55	23	18	10	35.87	6.78	1.56	15.66	4.36	0.278
		13:00	27	99	38	19	10	36.73	6.89	1.58	17.60	4.36	0.248
		14:00	28	143	52	20	20	33.79	6.51	1.60	18.63	4.06	0.218
		15:00	33	78	48	20	56	27.59	5.60	1.60	12.20	3.51	0.270
		16:00	31	83	56	19	31	18.97	4.08	1.58	11.11	2.58	0.232
		17:00	31	130	63	19	21	8.73	1.86	1.58	15.47	1.18	0.076
S4	26/01/2014	08:00	20	50	33	7	80	4.60	0.83	1.30	7.27	0.64	0.088
		09:00	21	35	28	11	60	15.89	3.46	1.39	6.735	2.50	0.371
		10:00	25	65	39	14	40	25.97	5.34	1.47	10.16	3.65	0.359
		11:00	21	46	24	18	35	34.12	6.56	1.56	10.05	4.21	0.419
		12:00	23	55	23	21	30	39.41	7.21	1.62	12.93	4.45	0.344
		13:00	20	96	35	22	35	40.88	7.38	1.65	13.60	4.46	0.328
		14:00	18	137	47	23	30	38.20	7.07	1.68	13.04	4.21	0.323
		15:00	23	72	43	21	30	31.95	6.26	1.62	9.56	3.85	0.403
		16:00	21	77	51	20	34	23.14	4.85	1.60	7.86	3.02	0.384
		17:00	21	125	58	19	20	12.64	2.76	1.58	11.10	1.75	0.158
S4	06/02/2014	08:00	21	36	28	8	80	6.03	1.20	1.33	6.67	0.90	0.136
		09:00	30	41	33	10	80	17.62	3.81	1.38	9.20	2.76	0.300
		10:00	34	70	44	14	75	28.06	5.67	1.46	13.53	3.88	0.287
		11:00	31	51	29	18	60	36.64	6.88	1.56	13.48	4.42	0.328
		12:00	32	60	28	19	34	42.32	7.53	1.58	16.68	4.76	0.285
		13:00	35	71	37	19	24	44.00	7.71	1.58	16.59	4.88	0.294
		14:00	33	62	44	19	24	41.26	7.42	1.58	11.43	4.70	0.411
		15:00	25	112	49	18	38	34.75	6.64	1.56	14.20	4.25	0.299
		16:00	24	161	69	18	40	25.63	5.28	1.56	13.53	3.39	0.251
		17:00	26	112	80	18	21	14.86	3.24	1.56	9.01	2.08	0.231
		18:00	26	114	113	17	44	3.07	0.43	1.52	6.48	0.28	0.044

Table 7: Measured concentrations, meteorological data, and derived rate constants and equilibrium parameter for roadside environment (site S5).

Site	Date	Time	O_3	NO	NO_2	T	Cld	Elevation	$J_{NO2}\times10^3$	$k_3\times10^{14}$	$10^{-11}\times([O_3]\,[NO]/[NO_2])$	$10^{-11}\times J_{NO2}/k_3$	ρ
			(ppb)	(ppb)	(ppb)	(°C)	(%)	Θ (°)	(s^{-1})	(cm^3 $molecule^{-1}$ s^{-1})	(molecule cm^{-3})	(molecule cm^{-3})	
S5	17/01/2015	08:00	25	20	23	5	78	15.04	3.28	1.26	5.50	2.60	0.473
		09:00	34	23	29	8	80	24.82	5.14	1.33	6.81	3.88	0.569
		10:00	34	31	28	10	94	32.63	6.35	1.37	9.29	4.63	0.499
		11:00	37	32	32	14	73	37.57	7.00	1.46	8.99	4.79	0.532
		12:00	36	50	37	16	51	38.79	7.14	1.50	11.93	4.76	0.399
		13:00	38	30	22	17	10	36.04	6.81	1.53	12.44	4.44	0.357
		14:00	29	29	21	19	20	29.87	5.95	1.58	10.18	3.77	0.370
		15:00	32	28	21	19	53	21.19	4.50	1.58	10.72	2.85	0.266
		16:00	37	15	14	19	37	10.84	2.36	1.58	9.19	1.49	0.162
S5	27/01/2015	08:00	28	21	32	6	28	4.74	0.87	1.28	4.71	0.68	0.144
		09:00	33	17	33	7	28	16.06	3.50	1.30	4.30	2.69	0.625
		10:00	31	26	30	7	58	26.15	5.37	1.30	6.48	4.11	0.635
		11:00	32	40	41	11	77	34.34	6.58	1.39	7.87	4.73	0.601
		12:00	32	41	41	14	60	39.64	7.24	1.46	7.75	4.95	0.639
		13:00	24	15	15	17	45	41.11	7.40	1.53	6.06	4.83	0.798
		14:00	39	24	19	18	40	38.41	7.10	1.56	12.42	4.56	0.367
		15:00	36	24	20	18	40	32.13	6.28	1.55	10.41	4.04	0.388
		16:00	37	23	14	17	55	23.28	4.88	1.53	14.89	3.18	0.214
		17:00	36	23	14	17	21	12.76	2.79	1.53	15.02	1.82	0.121
S5	17/02/2015	08:00	23	20	14	8	55	8.07	1.70	1.30	7.86	1.28	0.163
		09:00	33	30	24	12	60	19.94	4.26	1.40	9.97	3.03	0.304
		10:00	32	36	26	14	24	30.75	6.08	1.46	10.84	4.16	0.384
		11:00	35	23	22	16	40	39.75	7.25	1.51	8.74	4.81	0.550
		12:00	34	60	34	18	55	45.80	7.88	1.57	14.92	5.03	0.337
		13:00	35	42	28	18	50	47.58	8.04	1.56	12.51	5.17	0.413
		14:00	33	28	22	20	40	44.60	7.76	1.60	10.73	4.84	0.451
		15:00	32	15	15	20	45	37.67	7.01	1.61	7.93	4.34	0.547
		16:00	32	16	15	21	40	28.12	5.68	1.63	8.66	3.49	0.403
		17:00	29	17	14	21	35	16.98	3.68	1.63	8.84	2.26	0.256
		18:00	31	16	15	20	22	4.93	0.92	1.61	8.46	0.57	0.067

Table 8: Measured concentrations, meteorological data, and derived rate constants and equilibrium parameter for background site S6.

Site	Date	Time	O_3	NO	NO_2	T	Cld	Elevation	$J_{NO2}\times10^3$	$k_3\times10^{14}$	$10^{-11}\times([O_3]\,[NO]/[NO_2])$	$10^{-11}\times J_{NO2}/k_3$	ρ
			(ppb)	(ppb)	(ppb)	(°C)	(%)	Θ (°)	(s^{-1})	(cm^3 $molecule^{-1}$ s^{-1})	(molecule cm^{-3})	(molecule cm^{-3})	
		08:00	23	16	23	7	90	21.38	4.53	1.30	3.85	3.48	0.903
		09:00	25	18	23	11	88	32.39	6.32	1.40	4.57	4.53	0.990
		10:00	27	17	22	16	70	41.63	7.46	1.50	5.17	4.94	0.957
		11:00	32	16	23	17	63	47.89	8.07	1.53	5.29	5.26	0.996
S6	23/02/2015	12:00	37	15	25	19	87	49.72	8.22	1.57	5.46	5.22	0.956
		13:00	37	13	21	20	62	46.55	7.95	1.60	5.29	4.95	0.935
		14:00	33	12	24	20	38	39.33	7.20	1.60	4.34	4.49	1.034
		15:00	28	17	28	19	35	29.50	5.90	1.58	4.29	3.74	0.873
		16:00	19	19	26	19	32	18.16	3.92	1.58	3.49	2.48	0.710
		17:00	16	21	28	19	75	5.96	1.18	1.58	2.95	0.74	0.253
		08:00	20	16	21	15	80	21.64	4.58	1.48	3.71	3.08	0.831
		09:00	22	18	21	17	71	32.68	6.36	1.52	4.42	4.18	0.944
		10:00	22	17	20	17	70	41.96	7.49	1.53	4.64	4.89	1.054
		11:00	27	16	21	18	63	48.25	8.10	1.57	4.91	5.20	1.061
S6	24/02/2015	12:00	32	14	20	19	52	50.08	8.25	1.57	5.54	5.26	0.949
		13:00	32	13	20	19	40	46.88	7.98	1.58	5.05	5.05	1.000
		14:00	28	13	19	21	38	39.61	7.24	1.63	4.73	4.44	0.939
		15:00	26	13	23	22	35	29.73	5.93	1.65	3.69	3.60	0.975
		16:00	24	15	26	19	32	18.36	3.96	1.58	3.48	2.51	0.720
		17:00	11	15	28	21	18	6.13	1.22	1.63	1.46	7.52	0.515
		08:00	25	11	28	9	63	9.83	2.12	1.35	2.48	1.57	0.634
		09:00	28	15	29	13	60	21.90	4.63	1.45	3.59	3.20	0.890
		10:00	33	16	30	15	66	32.97	6.40	1.48	4.44	4.31	0.971
		11:00	33	16	26	16	49	42.29	7.53	1.58	4.98	4.99	1.003
		12:00	34	14	25	19	49	48.62	8.13	1.58	4.92	5.13	1.042
S6	25/02/2015	13:00	35	14	24	20	44	50.45	8.28	1.60	5.15	5.16	1.002
		14:00	35	14	24	20	34	47.21	8.01	1.60	5.24	4.99	0.952
		15:00	32	14	25	21	34	39.88	7.27	1.62	4.50	4.48	0.996
		16:00	29	14	27	21	29	29.96	5.97	1.63	3.65	3.66	1.004
		17:00	23	14	27	21	45	18.55	4.00	1.63	2.84	2.45	0.863
		18:00	13	16	29	20	50	6.29	1.26	1.60	1.73	7.90	0.458

Figure.2 shows for each site the time evolution of the PSS parameter ρ, derived from the concentrations measured at the different sites.

For the background site S6, the photostationary parameter ρ has a value of 1 during most of the daytime, with the exception of the first two and last two measurement points of the days. It has indeed been shown [1,18,24] that the equilibrium cannot be achieved in the morning and late afternoon hours due to the fast changes of the solar irradiance and of the rapid variations induced in the NO_2/NO ratio. Therefore, in the following discussion, only the behavior of ρ between 10:00 and 16:00 will be considered. The consistent value of 1 for site S6 during this period confirms that this site is sufficiently far from pollution sources, and that the photostationary hypothesis at this site is verified.

For the traffic sites S1 to S5, the situation is different, with the photostationary parameter ρ presenting a maximum during the noon hours of only 0.4 to 0.8, depending on the site and day of measurement. Only in two sites, S1 and S5, can we notice day to day variations, which can probably be ascribed to variations in the traffic conditions, and, in the case of the measurements taken on June 11, 2014 at Site 1, to the slightly different position of the analyzers compared to the other days.

4. Discussion

It is rare when the photostationary equilibrium is reached. Indeed, the calculation of ρ according to Equation 3 assumes that no other reaction can perturb the cycle of Reaction 1 to Reaction 3. However, reactions with other chemical components of the atmosphere can compete with reaction R3, such as in particular the reactions of NO with RO_2 or HO_2.

R4: $HO_2 + NO \rightarrow NO_2 + OH$; $k_4 = 9.7\times10^{-12}$ cm^3 $molecule^{-1}s^{-1}$ [25]

R5: $RO_2 + NO \rightarrow NO_2 + RO$; $k_5 = 9\times10^{-12}$ $cm^3 molecule^{-1}s^{-1}$ [15]

These reactions lead to the depletion of NO, and to an increase of NO_2 which will undergo photodissociation into $O(^3P)$ and an eventual increase of O_3 (reactions R1 and R2). The importance of the reactions of RO_2, HO_2 and CH_2O_3 with NO, has been previously reported, for instance by Bakwin et al. [26] with ρ values >5, by Hosaynali Beygi et al. [27] who found ρ>10, by Trebs et al. [17], with ρ>2.5, or by Ridley et al. [28], with ρ between 1.2 and 3. In a few studies, the deviation of ρ to unity has even been used to derive the concentration of radicals. For instance, Shetter et al. [18] estimated, using an average daytime of ρ~1.5, a peroxy radical concentration of 3×10^9 molecule cm^{-3}. Similarly, Rohrer et al. [24] calculated an upper limit concentration for RO_2 of 2.2×10^9 molecule cm^{-3} from the ρ value of 1.85 measured at noon. Others studies in moderately polluted atmospheres determined ρ values above 1, also linked to the RO_2 concentration [28-30]. More recently, simultaneous measurements of NO, NO_2, O_3, J_{NO2} and RO_2 were conducted by Matsumoto et al. [20] in Japan. They found values of ρ close to 1 but in some cases, ρ was significantly less than unity. They confirmed that the contribution of ROx is significant when the ozone concentration is low, with for instance ρ ~ 0.7 for a concentration ratio $RO_x/O_3 > 0.002$. They additionally suggested that the reaction rate constant of RO_2 with NO could be critical for the photostationary state to be reached. This effect is also noted in rural and remote zones, where values of ρ > 1 have been found (e.g.[17,31-33]) because the reactions of NO with oxidants are not significant enough.

Another parameter to consider is the importance of the influence of local emissions on the photostationary state, which remains a matter of further study. At the emissions, NO_X are mainly constituted by NO that is progressively transformed in NO_2 until the photo-stationary equilibrium is reached. For this reason, close to the source we expect the ratio $[NO][O_3]/[NO_2]$ to be higher than that corresponding to the equilibrium, i.e. J_{NO2}/k_3. In fact, two timescales must be taken into consideration. The first one is the timescale for turbulent transport τ_{turb}, which typically ranges from 1 to 10 sec at surface level [16]. The second one is the photochemical conversion time of NO into NO_2 (τ_{PSS}), typically of the order of 60 to 300 s [17,19,24]. The transport of the air masses is then much faster than the chemical conversion, which prevents reaching the photostationary equilibrium close to the sources [17]. In that case, ρ values below 1 would be expected. Only few studies however have found ρ values below 1. This has been observed by Eschenroeder and Martinez [34], who determined ρ values down to 0.3 in Los Angeles, by Kewley and Post [35], in Sydney, who observed values of ρ between 1 and 0.25 during the daytime when the UV intensity is high. Bilger [36] noted the same finding (ρ less than unity) and suggested that this could be due to the effect of mixing clean air and smog.

In the present study, we systematically found ρ values below 1, with the exception of the background site S6 where the photostationary state was reached. The photochemical conversion time of NO into NO_2 $\tau_{PSS}(S) = \frac{1}{J_{NO_2} + k_s \times [O_S]}$ (Trebs et al. 2012) was calculated in the range 50 to 95 s. The turbulent transport time was calculated according to (Trebs et al. 2006) as $\tau_{turb}(S) = k_{vk} \times (h_{mes} + h_0) \frac{u^*}{\sigma_w^2}$. We considered a value of 0.41 for the Von Karman coefficient k_{vk}, of 0.4 $m.s^{-1}$ for the friction velocity u^* [37], of 1.5 m for the roughness length h_0 [38], of 4 m for the height of measurement h_{mes}, and of 0.6 $m.s^{-1}$ for the standard deviation of the wind speed σ_w.

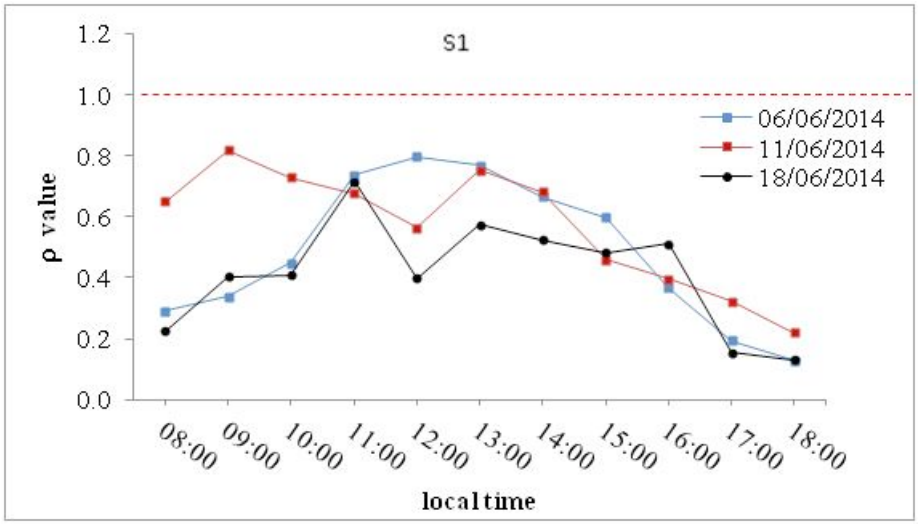

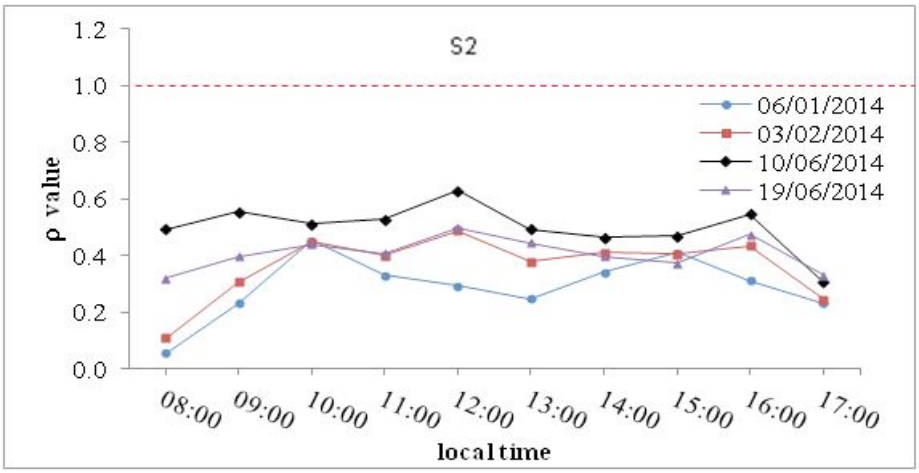

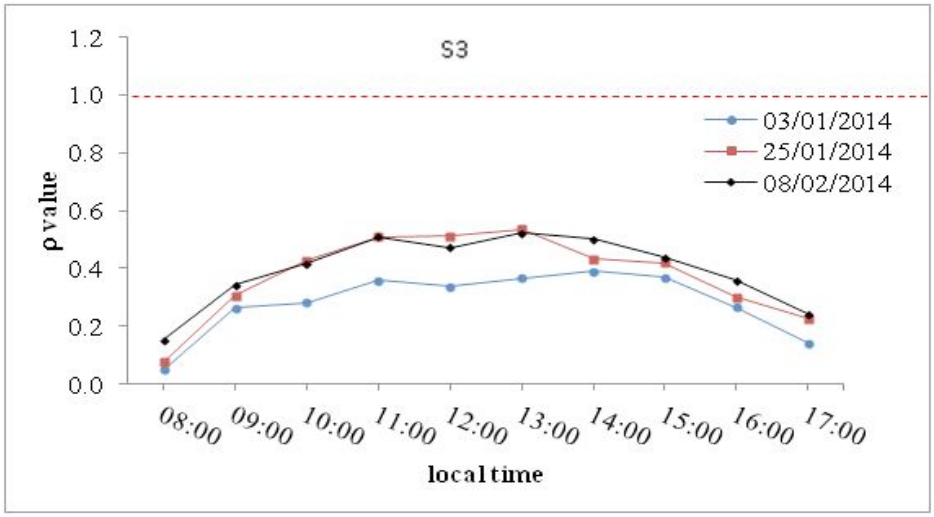

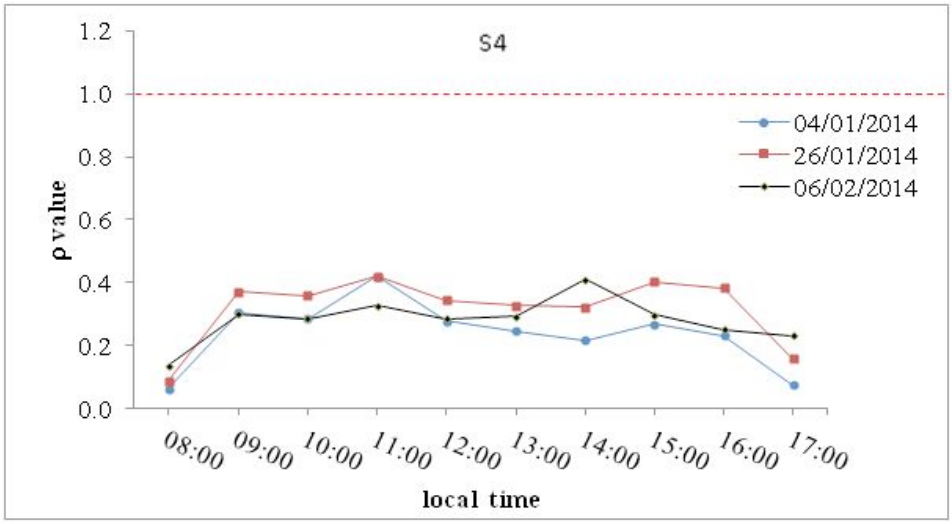

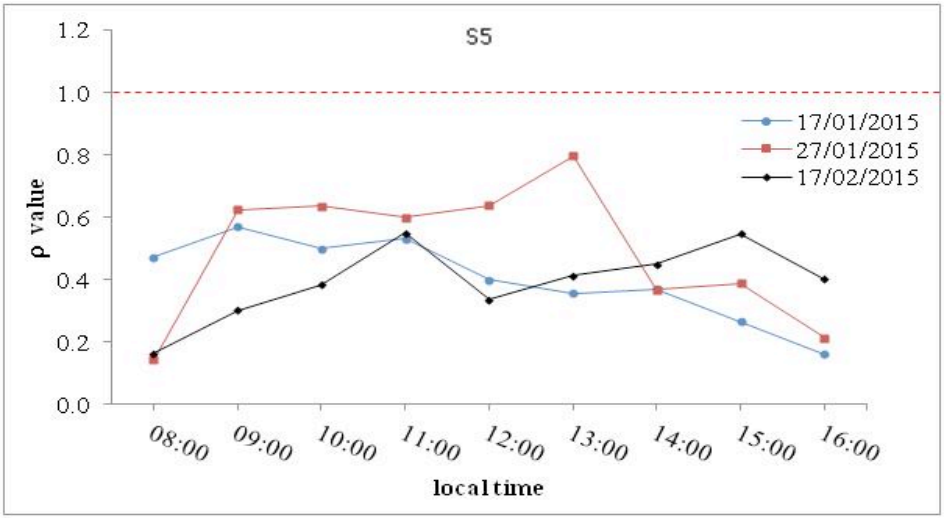

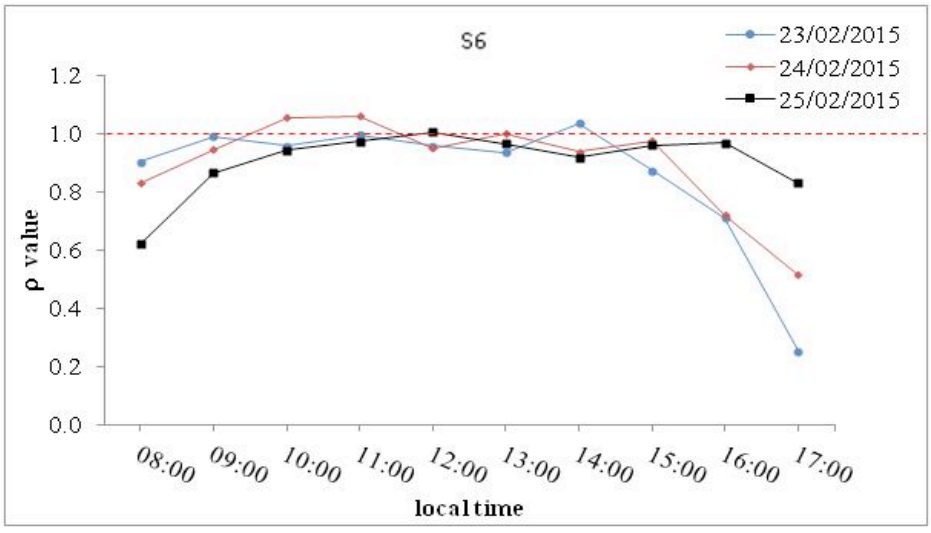

Figure. 2: Daily evolution of photostationary parameter ρ.

In these conditions, τ_{turb} varies between 0.5 and 3.5 s. It follows that the reaction of conversion of NO into NO_2 is slow compared to the transport phenomena, which prevents the photostationary state to be reached.
These values are reasonably in the same range as the ones previously reported in the literature and presented earlier in this article.

Sites S2, S3 and S4, present similar photochemical ratios for all the days of measurement, with only small differences that can probably be related to the intensity of the traffic. For site S1, stronger variations are

noted. It is however difficult to distinguish from ρ alone between the effect of the larger distance between the measurement point and the road axis, about 20 m on June 6 and 18, and 100 m on June 11, and the effect induced by fluctuations in the traffic conditions or by the wind speed and direction. A closer inspection of the data reported in Table 3 shows indeed that when the distance between the source, i.e. the road, and the measurement point increases, the observed NO concentration is reduced by a factor 2, but that at the same time, NO_2 concentration also decreases, confirming that both effects, the chemical reactivity and the dispersion of pollutants by the wind, are of the same order in these conditions. This is also the case at site S5, where in addition the absence of nearby tall buildings induces a rapid dispersion of the pollutants, as evidenced by the relatively low concentration of nitrogen oxides in spite of the heavy traffic.

A plot of the value of ρ as a function of the observed concentration ratio NO_2/NO is given on Figure. 3. For the background site, this plot translates as a constant, as expected when the photostationary state is reached. For the traffic sites, the ρ value is directly and linearly correlated to the ratio, with a threshold between the two regimes for NO_2/NO ~1.4 in our conditions, that is with a background ozone concentration of 30 to 35 ppb, as measured in site S6. This limit value of 1.4 is linked to the excess NO directly emitted by the vehicles, before reaction into NO_2 or dispersion of the air masses. Such a plot would allow for a quick determination whether the photostationary state is reached in any urban environment.

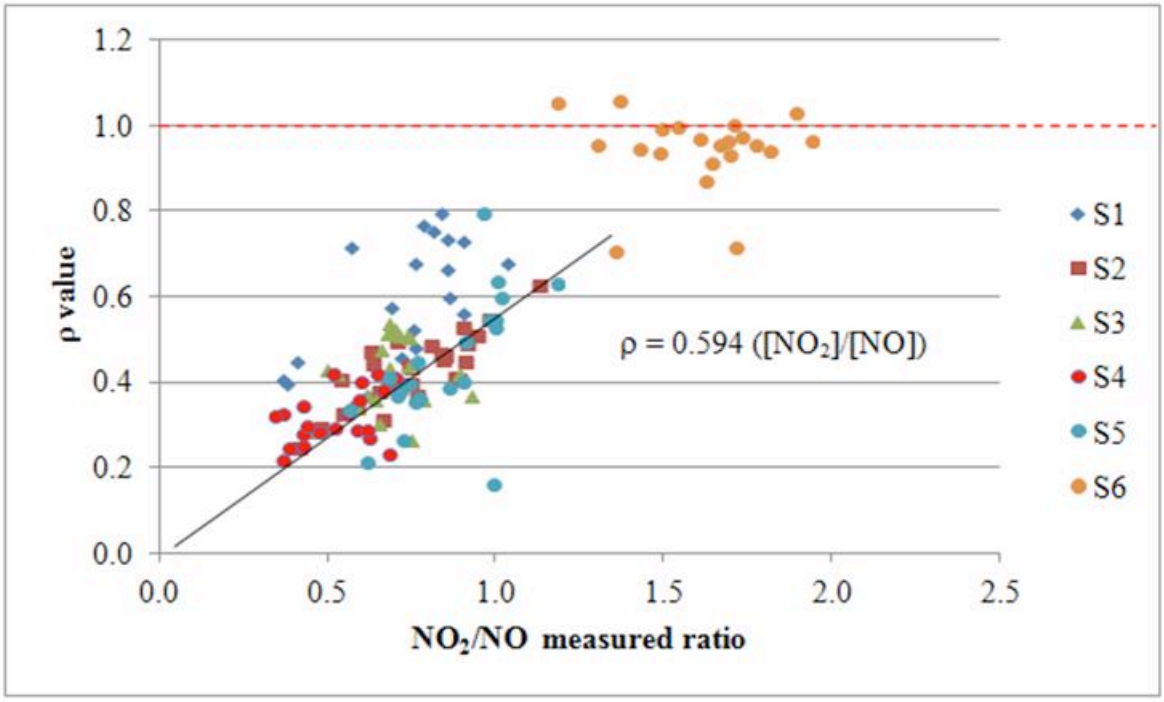

Figure. 3: Evolution of the photostationary parameter ρ with the NO_2/NO ratio

5. Conclusion

In this work, we measured the NOx and O_3 concentrations in different roadsides places, and one background site, in the city of Agadir, Southern Morocco, between January 2014 and June 2015. The observed concentrations range between 13 and 42 ppb for ozone, 15 and 252 ppb for NO, and 14 and 113 ppb for NO_2. From this large dataset, we investigated whether the assumption that the photostationary state was reached, implicitly used in the air quality predictive models, was holding true. To our knowledge, this is the first time that this assumption is tested in roadside environments. Only in the background site, far from the direct traffic emissions, could the atmosphere considered in photostationary equilibrium. For the sites close to the traffic, the excess NO from the tailpipe emissions do not have time to react or to be perfectly mixed with the background pollutants, leading to a significant deviation from the photostationary equilibrium. We suggest that the measured concentration ratio NO_2/NO may be used as a criterion to evaluate the photostationary state of the urban atmosphere, which could be taken into account both for field measurements and for modeling purposes.

Acknowledgments

The authors thank the Agadir Urban Community for financial support (Agadir BHNS project 2013-2015) and Dr. J. Damich for technical and logistic assistance. The authors thank also the local authorities

(Wilaya) for their collaboration. This work was made possible thanks to the scientific equipment donated to the group of Materials and Physical Chemistry of the Atmosphere and Climate of the Faculty of Science of Ibn Zohr University by the PC2A laboratory (University of Lille 1, France) and by Lig'Air (Orléans, France).

References

1. Carpenter,L.J.;. Clemitshaw, K.C. Burgess R.A,. Penkett, J.N. Cape and G.G Mcfadyen. Investigation and evaluation of the NOx/O3 photochemical steady state S.A. Atmos. Environ. 32(19) (1998) 3353-3365.
2. S. Sillman. The relation between ozone, NOx and hydrocarbons in urban and polluted rural environments. Atmos. Environ. 33, (1999) 1821-1845.
3. L. Ntziachristos and Z. Samaras. Speed-dependent representative emission factors for catalyst passenger cars and influencing parameters. Atmos. Environ. 34 (2000) 4611-4619.
4. C. Liu and D.Y.C Leung. Numerical study on the ozone formation inside street canyons using a chemistry box model. J. Atmos. Sci. 20 (2008) 832-837.
5. C. Mensink and G. Cosemans. From traffic flow simulations to pollutant concentrations in street canyons and backyards. Environ. Model. Soft. 23 (2008) 288-295.
6. J. Baker, H.L. Walker and X. Cai. A study of the dispersion and transport of reactive pollutants in and above street canyons – a large eddy simulation. Atmos. Environ. 38, (2004) 6883-6892.
7. S. Vardoulakis, M. Valiantis, J. Milner and H. ApSimon, Operational air pollution modeling in the UK-Street Canyon applications and challenges. Atmos. Environ. 41 (2007) 4622-4637.
8. M. Hirtl and K. Baumann-Stanzer. Evaluation of two dispersion models (ADMS-Roads and LASAT) applied to street canyons in Stockholm, London and Berlin. Atmos. Environ. 41 (2007) 5959-5971.
9. P.A. Leighton. *Photochemistry of Air Pollution*. Academic, San Diego, California (1961).
10. J.H. Seinfeld. *Atmospheric Chemistry and Physics of Air Pollution*. Wiley, New York (1986).
11. R. Atkinson. Kinetics and mechanisms of the gas-phase reactions of the hydroxyl radical with organic compounds. J. Phys. Chem. Reference Data, Monograph. 1 (1989) 1-246.
12. Y. Bedjanian, G. LeBras and G. Poulet. Kinetics and mechanism of the IO + BrO reaction. J. Phys. Chem. A 102 (1998) 10501-10511.
13. R. Dickerson, D. Stedman and A. Delan. Direct Measurements of Ozone and Nitrogen Dioxide Photolysis Rates in the Troposphere. J. Geophys. Res. 87 (1982) 4933-4946.
14. F. Kasten and G. Czeplak. Solar and terrestrial radiation dependent on the amount and type of cloud. Solar. Energy. 24 (1980) 177-189.
15. R. Atkinson , D.L. Baulch, R.A. Cox, J.N. Crowley, R.F. Hampson, R.G. Hynes, M.E. Jenkin, M.J. Rossi and J. Troe. Evaluated kinetic and photochemical data for atmospheric chemistry: Volume I Gas phase reactions of Ox, HOx, NOx and SOx species. Atmos. Chem. Phys. 4 (2004) 1461-1738.
16. I. Trebs, L.L. Lara, M. Zeri, L.V. Gatti, P. Artaxo, R. Dlugi, J. Slanina, M.O. Andreae and F.X. Meixner. Dry and wet deposition of inorganic nitrogen compounds to a tropical pasture site (Rondonia, Brazil). Atmos. Chem. Phys. 6 (2006) 447-469.
17. I. Trebs, O.L. Mayol-Bracero, T. Pauliquevis, U. Kuhn, R. Sander, L. Ganzeveld, F.X. Meixner, J Kesselmeier, P. Artaxo and M.O. Andrea. Impact of the Manaus urban plume on trace gas mixing ratios near the surface in the Amazon Basin: Implications for the NO-NO2-O3 photostationary state and peroxy radical levels. J. Geophys. Res.117, D05307 (2012).
18. R.E. Shetter, D.H. Stedman and D.H. West. The NO/NO2/O3 Photostationary State in Claremont, California. J. Air. Pollut. Contr. Assoc. 33 (3) (1983) 212-214.
19. J. Yang, R. E. Honrath, and M. C. Peterson, Photostationary state deviation-estimated peroxy radicals and their implications for HOx and ozone photochemistry at a remote northern Atlantic coastal site. J. Geophys. Res. 109, D02312 (2004).
20. J. Matsumoto, N. Kosugia, A. Nishiyama, R. Isozaki, Y. Sadanaga, S. Kato, H. Bandow and Y. Kajii. Examination on photostationary state of NOx in the urban atmosphere in Japan. Atmos. Environ. 40 (2006) 3230-3239.
21. High Commission for Planning (HCP). General Census of Population and Habitat, Morocco (2014).
22. A. Ait Taleb, A. Saghi, A. El Hammadi, S. Le Calvé, L. El Maimouni. Atmospheric levels of formaldehyde, acetaldehyde and benzaldehyde in an industrial site, Anza (northwest of Agadir, Morocco). J. Environ. Sci. Eng. A1 (2012) 776-784.

23. Z. Ouabourrane, M. El Abassi, H. El Haddaj, Lh. Bazzi, B. Hanoune, L. El Maimouni. BTX and carbonyl compounds in the roadside environment of Inezgane-Ait Melloul (southwestern Morocco). J. Environ. Sci. 8 (2017) 611-621.
24. F. Rohrer, D. Brüning, E.S. Grobler, M. Weber and D.H. Ehhalt. Mixing Ratios and Photostationary State of NO and NO2 Observed During the POPCORN Field Campaign at a Rural Site in Germany. J. Atmos. Chem. 31 (1998) 119-137.
25. B. Bohn and C. ZetzschRate constants of HO2 + NO covering atmospheric conditions. 1. HO2 formed by OH + H2O2. J. Phys. Chem. A. 101, (1997) 1488-1493.
26. P.S. Bakwin, S.C. Wofsy and S.M. Fan. Reactive Nitrogen-Oxides and Ozone above a Taiga Woodland. J. Geophys. Res. 99(D1) (1994) 1927-1936.
27. Z. Hosaynali Beygi, H. Fischer, H.D. Harder, M. Martinez, R. Sander, J. Williams, D.M. Brookes, P.S. Monks and J. Lelieveld. Oxidation photochemistry in the Southern Atlantic boundary layer: unexpected deviations of photochemical steady state. Atmos. Chem. Phys. 11 (2011) 8497-8513.
28. B.A. Ridley, S. Madronich, R.B. Chatfiled, J.G. Walega, R.E. Shetter, M.A. Carroll and D.D. Montzka. Measurements and Model Simulations of the Photostationary State during the Mauna Loa Observatory Photochemistry Experiment: Implications for Radical Concentrations and Ozone Production and Loss Rates. J.Geophys. Res. 97, (1992) 10375-10388.
29. K. Mannschreck, S. Gilge, C. Plass-Duelmer, W. Fricke and H. Berresheim. Assessment of the applicability of NO-NO2-O3 photostationary state to long-term measurements at the Hohenpeissenberg GAW Station, Germany. Atmos. Chem. Phys. 4 (2004) 1265-1277.
30. A. Volz-Thomas, H. Geiss and A. Hofzumahaus, Introduction to Special Section: Photochemistry Experiment in BERLIOZ. J. Geophys. Res.108 (D4) (2003) 8252.
31. C.A. Cantrell, R.E. Shetter, J.G Calvert, D.D. Parrish, F.C. Fehsenfeld, P.D. Goldan, W. Kuster, E.J. Williams, H.H. Westberg, G. Allwine and R. Martin. Peroxy radicals as measured in ROSE and estimated from photostationary state deviations. J. Geophys. Res. 98 (1993) 18355-18366.
32. D.A. Hauglustaine, S. Madronich, B.A. Ridley, S.J. Flocke, C.A Cantrell, F.L. Eisele, R.E. Shetter, D.J. Tanner, P. Ginoux and E.L. Atlas. Photochemistry and budget of ozone during the Mauna Loa Observatory Photochemistry Experiment (MLOPEX 2). J. Geophy. Res. 104(D23) (1999) 30275-30307.
33. D.A. Hauglustaine, S. Madronich, B.A. Ridley, J.G. Walega, C.A Cantrell and R.E. Shetter. Observed and model-calculated photostationary state at Mauna Loa Observatory during MLOPEX 2. J. Geophys. Res.101(D9) (1996) 14681-14696.
34. A.Q. Eschenroeder and J.R. Martinez. Analysis of Los Angeles atmospheric reaction data from 1968 and 1969. Final report CRC-APRAC Project No. CAPA-7-68. Gen. Res. Corp. CR-l-170 (1970).
35. D.J. Kewley and K. Post. Photochemical ozone formation in the Sydney airshed. Atmos. Environ. 12 (1978) 2179- 2184.
36. R.W Bilger. The effect of admixing fresh emissions on the photostationary state relationship in photochemical smog. Atmos. Environ. 12 (1978) 1109-1118.
37. J.R. Garratt. *The atmospheric boundary layer*, Cambridge, 315. Cambridge University Press (1992).
38. G.J. McRae, W.R. Goodin, J.H. Seinfeld. Development of a second-generation mathematical model for urban air pollution _I. Model formulation. Atmos. Environ. 16(4) (1982) 679-696.